

Placement of data transmission equipment in the flood warning system based on the Internet of Things (case study : Jiroft Dam Basin)

Marzieh Mohseni ^{*1}, Amineh Naseri ², Leila Sheikhmamoo ¹

1. Department of Civil Engineering, Sirjan University of Technology, Sirjan, Iran.
2. Department of Computer Engineering, Sirjan University of Technology, Sirjan, Iran.

ABSTRACT

Floods are one of the most damaging natural disasters that have increased in frequency, severity and resulting damages in recent years in Iran and around the world. One solution to reducing flood damages is to develop a flood monitoring and management system to quickly and widely communicate information and warnings to residents. Conventional methods of flood monitoring cannot provide rapid and widespread community notification. As a solution, this study focuses on an Internet of Things-based flood warning system, which is an intelligent technology capable of sending real-time information using smartphones and web services. Jiroft dam basin has been chosen for the implementation of this system. A key challenge in establishing Internet of Things-based flood warning systems lies in the strategic distribution of equipment for data collection and transmission. To address this, a hexagonal algorithm was employed for equipment placement in this study. By identifying the most flood-prone areas within the basin through the use of the K-means clustering algorithm and flood index(f), the study reveals the efficacy of combining these tools in determining flood potential and optimal locations for implementing flood warning systems. Following the identification of sensitive points within the basin, the study selects the Maidan sub-basin as the most susceptible to floods. Through the application of the hexagonal algorithm and a WSN-03 module with a 3.5-kilometer data transmission range, 192 suitable locations for equipment installation are pinpointed for data reception and transmission. This study will be useful for the development of early flood warning systems and reservoir management.

KEYWORDS

Hexagonal algorithm, K-means clustering algorithm, Curve number, Time of concentration.

1. Introduction

Floods are among the most destructive natural disasters, and in recent years, their frequency, intensity, and associated damages have increased in Iran and other parts of the world. A review of the history of floods in Iran reveals two main factors contributing to severe and destructive flooding. The first factor is the presence of the Zagros Mountain Range in the southwest and the Alborz Mountain Range in the northeast of Iran. Both ranges act as barriers to air flow, causing rain to accumulate on the windward sides, while central Iran remains dry. The second factor is a combination of soil type, land use, and slope, which results in minimal water infiltration and leads to sudden flash floods during rainfall [1]. These conditions have made floods the second most common natural hazard in Iran after earthquakes[2].

*Corresponding Author:

Marzieh Mohseni,

Email: mohseni_m@sirjantech.ac.ir

Received: 2024.12.08

Accepted: 2025.02.16

J. Hydraul. Struct., 2025; 11(4):33-46

DOI: 10.22055/jhs.2025.48451.1331

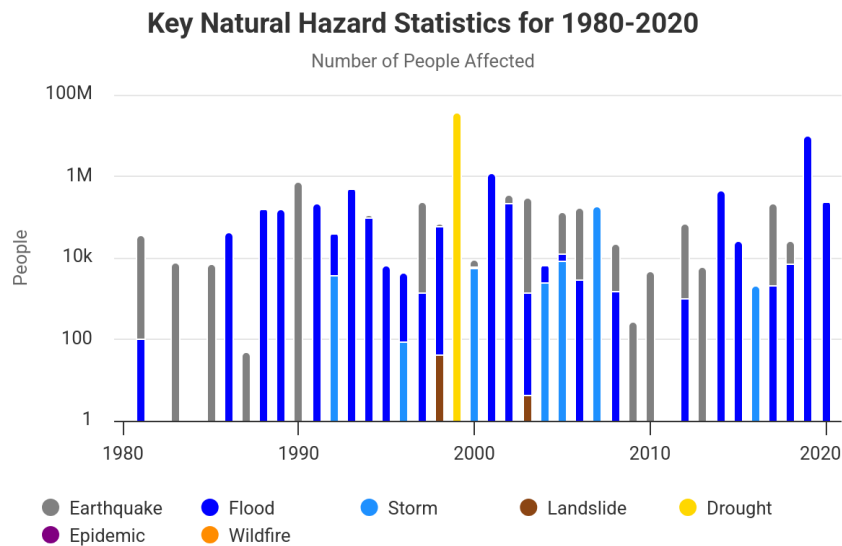


Figure 1. Main hazard risks to Iran, measured by number of people affected, for the period 1985-2020 [2]

In recent years, Iran has experienced numerous floods. For instance, in August 2001, floods in Golestan Province claimed 247 lives, and in 1986, at least 200 people lost their lives due to flooding [1].

Early and widespread flood warnings, which provide sufficient time for evacuation and property protection, are proposed as an effective solution for reducing damages and casualties. However, this is not feasible with conventional methods. In traditional approaches, warnings are often based on visual monitoring. For example, in East Java, Indonesia, each dam in Banyuwangi has a supervisor responsible for monitoring and reporting water conditions. This method is neither efficient nor practical, as the supervisor must remain in the location 24 hours, and there is no guarantee of timely and accurate information transmission [3]. As such, the development of early warning systems in developing countries faces significant technological, social, and political challenges. Additionally, the maintenance and operation of such systems by non-experts present further difficulties. Consequently, developing countries often experience far greater losses and destruction from floods compared to developed countries[4].

In flood warning detection systems, two

critical factors are flood detection accuracy and the speed of data collection and transmission. One of the latest techniques for data transmission is the Internet of Things (IoT) [5]. IoT facilitates the control and connection of multiple objects via the internet. The architecture of these networks offers reliability and efficiency. Additionally, due to their minimal need for specific environmental infrastructure, ease of deployment, low energy consumption, and cost, as well as high scalability and customization based on specific measurement needs, they are highly effective [6].

Ancona et al.[7] studied the history of using IoT and wireless smart sensor networks to enhance the reliability and efficiency of flood monitoring systems. In their study, data collected from local cameras and citizen reports were transmitted via the internet to software systems, which then analyzed the data using an alert planning system. Based on the risk level, warning messages were sent to citizens.

Udo and Isong[8] described flood monitoring and detection using a wireless sensor network, where variables such as water level, rainfall intensity, relative humidity, and temperature were employed to monitor and assess flood severity. Flood

intensity was classified qualitatively as low, medium, or high, and warnings were sent to residents in the affected area. Studies by Mousa et al. [9], Madhumathi and Grace[10], and Hartono et al. [11] focused on detecting flash floods using ultrasonic and infrared sensors. Azid et al. [12] used pressure sensors to monitor water levels, sending SMS alerts when water levels exceeded predefined thresholds.

Shah et al. [13] utilized a Raspberry Pi board to collect flood data and a GSM module to send SMS alerts. Their study was conducted in a simple laboratory environment without calculating warning thresholds. Andrade and Oishi [14] recommended using SMS in wireless sensor networks (WMSNs) as a relatively simple and cost-effective method for transmitting information during natural disasters and emergencies.

In flood prediction systems designed by Mitra et al.[15] and Bande and Shete [16], data were collected using sensors, analyzed using artificial neural networks, and communicated via IoT. Citizens were alerted about flood occurrence and warnings through smartphones and internet networks.

Shalini et al.[17] focused on remote monitoring of water levels using wireless sensor networks and sending alerts through SMS, television, and radio, though they emphasized the possibility of delayed warnings.

In the flood monitoring and tracking system developed by Yuliandoko et al.[3], water depth data were processed to detect floods and assess risk levels. The risk level was directly sent from the monitoring center to residents in flood-prone areas, enhancing early flood detection. Zahir et al.[18] proposed a smart flood monitoring and control system for urban and rural areas with low cost and easy maintenance, transmitting information to users via the internet and SMS.

A key challenge in flood monitoring using IoT devices is the effective distribution of data collection and transmission equipment to avoid sensor data overlap. Over-installing IoT devices increases capital

and maintenance costs and generates redundant data. Conversely, under-installing IoT devices may result in insufficient data collection for all flood parameters across different geographical locations, adversely affecting and reducing forecasting accuracy. On the other hand, determining the optimal number of IoT devices prevents investment wastage and ensures the collection of necessary data for effective flood monitoring.

Most studies have focused on equipment connectivity and notification mechanisms, with limited research on the optimal placement of IoT devices. In this regard, reference can be made to the study by Sood et al.[6] in which a hexagonal algorithm was proposed for the deployment of IoT equipment in a hypothetical environment with dimensions of 200 meters, with each basin approximately 1 meter. Jiroft watershed is one of the flood-prone areas in the country due to its dry and desert climate conditions. The presence of heavy rainfall events produces significant floods that are a major concern for the inhabitants of the region [19]. In the present study, by considering an IoT-based flood prediction and warning system in Jiroft dam basin, the placement of IoT equipment using the hexagonal algorithm has been addressed.

2. Data, Methods and Models

2.1. Study sites and data

Jiroft dam is one of the largest concrete dams in Iran, located approximately 40 kilometers northwest of the city of Jiroft on the Halil River. The Jiroft dam basin, located in the southeast of Iran, formed the study area. The basin lies between geographical coordinates of $28^{\circ} 00' 0''$ – $29^{\circ} 58' 0''$ N latitude and $56^{\circ} 29' 0''$ – $58^{\circ} 58' 0''$ E longitude (Fig.2). The basin drainage area covers approximately 5000 km². The average annual rainfall in Jiroft basin is over 220 millimeters, reaching over 400 millimeters in the surrounding mountainous areas[20]. Due to the intensity of rainfall and the mountainous nature of the Jiroft watershed, floods occur frequently every year. Figure 2 shows the geographical

location of Jiroft county on the map of Iran and Kerman province, as well as the watershed of the Jiroft Dam.

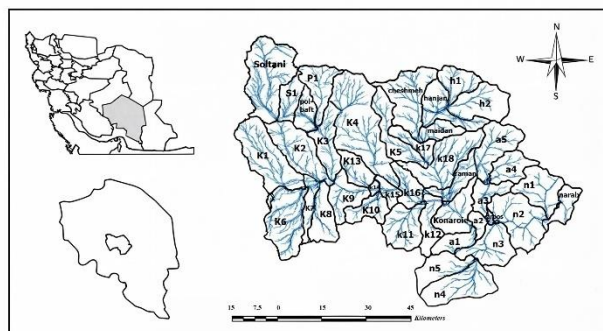


Figure 2. Graphical location of the city of Jiroft (filled by gray color) and geographical location of Jiroft dam basin and division of sub-basins [19].

The Jiroft dam basin has been divided into 43 sub-basins. The characteristics of each sub-basin, are presented in Table 1.

Table 1. Characteristics of the sub-basins of the Jiroft dam basin

| No. | Sub-basin | Slope(%) | Area of subbasin(km ²) | No | Sub-basin | Slope(%) | Area of subbasin(km ²) |
|-----|-----------|----------|------------------------------------|----|-----------|----------|------------------------------------|
| 1 | a1 | 0.02 | 78.9 | 23 | k20 | 0.72 | 8.3 |
| 2 | a2 | 0.73 | 34.4 | 24 | k3 | 0.29 | 142.5 |
| 3 | a3 | 0.53 | 93.2 | 25 | k4 | 0.14 | 446.5 |
| 4 | a4 | 0.07 | 112.4 | 26 | k5 | 0.16 | 155.4 |
| 5 | a5 | 0.12 | 175.5 | 27 | k6 | 0.13 | 244.5 |
| 6 | aroos | 0.74 | 10.4 | 28 | k7 | 0.47 | 72.3 |
| 7 | cheshmeh | 0.05 | 254.9 | 29 | k8 | 0.36 | 128.4 |
| 8 | H1 | 0.03 | 107.7 | 30 | k9 | 0.13 | 128.3 |
| 9 | h2 | 0.02 | 181.5 | 31 | konaroi | 0.17 | 146.9 |
| 10 | hanjan | 0.09 | 156.1 | 32 | maidan | 0.12 | 67.8 |
| 11 | k1 | 0.12 | 287.7 | 33 | n1 | 0.18 | 165.5 |
| 12 | k10 | 0.06 | 94 | 34 | n2 | 0.15 | 242.6 |
| 13 | k11 | 0.06 | 167.5 | 35 | n3 | 0.02 | 163.2 |
| 14 | k12 | 0.32 | 108 | 36 | n4 | 0.02 | 23.1 |
| 15 | k13 | 0.3 | 88.9 | 37 | n5 | 0.02 | 13.2 |
| 16 | k14 | 0.13 | 12.7 | 38 | narab | 0.38 | 80.8 |
| 17 | k15 | 0.3 | 48.6 | 39 | p1 | 0.13 | 95.4 |
| 18 | k16 | 0.3 | 91.4 | 40 | pol-baft | 0.19 | 71.7 |
| 19 | k17 | 0.2 | 67.4 | 41 | raman | 0.3 | 140.1 |
| 20 | k18 | 0.19 | 284.4 | 42 | s1 | 0.26 | 76.9 |
| 21 | k19 | 0.72 | 19.1 | 43 | soltani | 0.08 | 338.9 |
| 22 | k2 | 0.16 | 217.2 | | | 0.72 | 8.3 |

2.2. Internet of Things (IoT)

The Internet of Things is a tool for collecting, filtering, and analyzing data. These data come from sources such as remote sensing, smart cameras, smart buoys, smart sensors, water level sensors, and more. After collecting the data, the Internet of Things filters and analyzes the information, providing a comprehensive view of the extent of flooding and the time of its occurrence. This process informs the community of potential dangers without wasting time [21].

2.2.1. Location of IoT Devices

One of the main challenges in monitoring floods using IoT devices is the appropriate distribution of equipment for receiving and sending data in a way that sensor data do not overlap. Determining the appropriate number of IoT transmission devices prevents investment waste and collects the necessary data for effective flood monitoring. If a small

number of IoT devices are installed, they will not be able to collect all the information related to flood parameters for each geographical location, thus reducing the accuracy of the system's predictions. Conversely, installing too many IoT devices increases capital, repair, and maintenance costs and generates additional data. In the present study, a hexagonal algorithm was used for the appropriate location of IoT equipment. The advantage of using hexagonal shapes is that no area is left uncovered, and the distance from the center of one hexagon to the center of another hexagon is equal. An example of the proposed structure is shown in figure 3. The origin coordinates and axes are clearly indicated in this figure. In this two-dimensional coordinate system, the origin coordinates are the most sensitive area in the watershed to flooding, the x-axis is in the direction of the slope of the watershed, and the y-axis is in the direction of the width of the watershed.

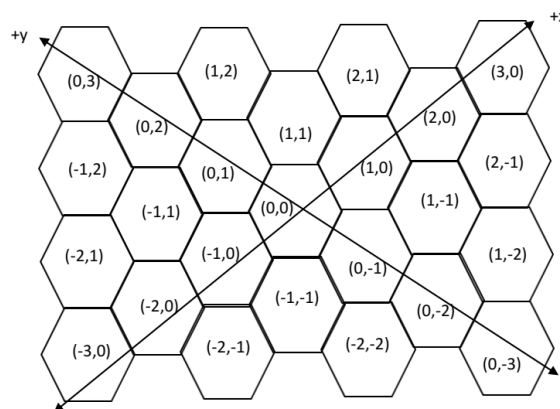


Figure 3. Implementation of the hexagonal algorithm[6]

The implementation of the hexagonal algorithm in the study area is presented in algorithm 1. In algorithm 1, it is assumed that each IoT device covers a hexagonal area with a radius R (the coverage radius of data transmission and reception equipment) to collect data at the desired rate and improve data transfer speed for processing. The size of the hexagon and the number of IoT devices to be installed are interdependent, the number of hexagons is determined based

on the coverage area of IoT devices. In other word, the radius of the hexagons is selected according to the board of the receiving and transmitting modules, This means that, with an increase or decrease in the radius of each module's board, the selected radius of each hexagon and consequently the number of hexagons will also change. For example, in this study, a WSN-03 module with a board of 3.5 kilometers has been considered, which will cover an area of approximately 31.85

km². If a module with a different board is used, this coverage area will certainly

change, resulting in a corresponding variation in the number of devices required.

Algorithm1. The hexagon division algorithm of the geographical area is as follows:

Step 1: Choose the most sensitive watershed area in flood formation as the origin.
 Step 2: Set the axis directions:
 x-axis from the highest point in the watershed (+x) to the lowest point in elevation (-x)
 y-axis: width of the watershed.
 Step 3: Set the radius of each hexagon to half the device length ($R/2$) for each hexagon center to have the same distance.
 Step 4: Install each IoT device at the center of the hexagon to cover the radius area ($R/2$) and obtain the coordinates of the hexagon centers.
 Step 5: Record the latitude and longitude of the origin coordinates for geographical reference and obtain the geographical locations of the hexagon centers.

2.3. Flood potential of the Jiroft dam sub-basins

The first step in algorithm 1, is to determine the most sensitive point to floods in the desired watershed. In this section, the determination of the flood potential of the watershed is addressed. Different indicators are used to identify locations with high flood potential. Among the most important and practical indicators used in this regard are the $F\%$ and f index, which work based on peak discharge extracted from mathematical models. These indicators have been used in various studies, such as the study by Solaimani Sarood et al. [19]. In this study, the Jiroft dam basin is divided into 43 sub-basins, and using the HEC-HMS precipitation-runoff model and RS, GIS techniques, the $F\%$ and f indicators are calculated. To achieve this, the curve number must first be estimated. In order to determine the curve number in the sub-basins, a soil

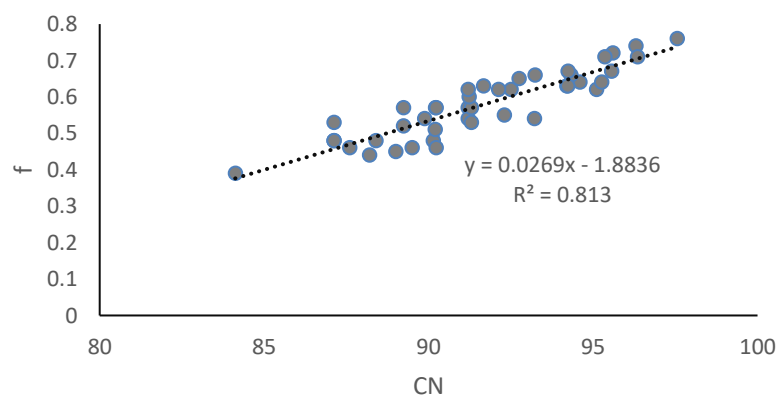
texture map of the area was initially prepared. Subsequently, using hydrological soil group tables, a hydrological soil map was created. Based on this hydrological soil map, the majority of the area is classified into groups B and C. In the next step, utilizing satellite images and remote sensing techniques, a land use map of the area was produced. The results indicated that a significant portion of the area consists of rock-bare soil, which have a high potential for flooding. Following this, by integrating the hydrological soil map and the land use map, a curve number (CN) map for the watershed was drawn. It should be noted that the findings of Solaimani Sarood et al. [19] were also utilized in these cases. The estimated values for each sub-basin are presented in table 2.

Table 2. Flood index values for the hydrological units of Jiroft dam basin

| No. | Sub-basin | CN | f | F (%) | No | Sub-basin | CN | f | F (%) |
|-----|-----------|------|------|-------|----|-----------|------|------|-------|
| 1 | a1 | 82.1 | 0.57 | 2.7 | 23 | k20 | 77 | 0.54 | 0.27 |
| 2 | a2 | 81.3 | 0.55 | 1.14 | 24 | k3 | 77.1 | 0.52 | 4.47 |
| 3 | a3 | 90.1 | 0.62 | 3.47 | 25 | k4 | 78.1 | 0.6 | 16.12 |
| 4 | a4 | 87.1 | 0.48 | 3.24 | 26 | k5 | 91.1 | 0.67 | 6.29 |
| 5 | a5 | 82.1 | 0.54 | 5.73 | 27 | k6 | 94.1 | 0.76 | 11.18 |
| 6 | aroos | 78 | 0.46 | 0.29 | 28 | k7 | 88.1 | 0.63 | 2.72 |
| 7 | cheshmeh | 75.2 | 0.48 | 7.37 | 29 | k8 | 90.1 | 0.64 | 4.98 |
| 8 | H1 | 73.1 | 0.46 | 2.99 | 30 | k9 | 92.1 | 0.71 | 5.53 |
| 9 | h2 | 75 | 0.44 | 4.86 | 31 | konaroi | 84.1 | 0.62 | 5.49 |
| 10 | hanjan | 92 | 0.74 | 7.01 | 32 | maidan | 90.1 | 0.71 | 2.9 |
| 11 | k1 | 84.1 | 0.62 | 10.79 | 33 | n1 | 82.1 | 0.62 | 6.18 |
| 12 | k10 | 88 | 0.64 | 3.65 | 34 | n2 | 78.1 | 0.57 | 8.42 |
| 13 | k11 | 93.1 | 0.57 | 5.81 | 35 | n3 | 77.2 | 0.57 | 5.58 |
| 14 | k12 | 78.1 | 0.51 | 3.31 | 36 | n4 | 74.1 | 0.53 | 0.74 |
| 15 | k13 | 88.1 | 0.55 | 2.98 | 37 | n5 | 67.8 | 0.39 | 0.31 |
| 16 | k14 | 84.3 | 0.54 | 0.42 | 38 | narab | 74.4 | 0.48 | 2.34 |
| 17 | k15 | 82.1 | 0.53 | 1.56 | 39 | p1 | 73.2 | 0.48 | 2.77 |
| 18 | k16 | 76.5 | 0.45 | 2.5 | 40 | pol-baft | 87.1 | 0.67 | 2.91 |
| 19 | k17 | 78.5 | 0.46 | 1.88 | 41 | raman | 83.1 | 0.63 | 5.32 |
| 20 | k18 | 91.1 | 0.72 | 12.47 | 42 | s1 | 84.2 | 0.66 | 3.06 |
| 21 | k19 | 88.1 | 0.66 | 0.77 | 43 | soltani | 84.5 | 0.65 | 13.24 |
| 22 | k2 | 79.2 | 0.57 | 7.43 | | | | | |

The results of this study showed that the values extracted using the f indicator have a correlation coefficient of 0.813 with the curve number values (CN), such that the f

indicator values change linearly with the change in curve numbers, as shown in figure 4.

**Figure 4. Relationship between curve number (CN) and f indicator values**

In the Saghafian and Farazjou[22] study, the researchers highlighted the importance of incorporating concentration time into flood warning projects, alongside flood indicators. The study of the Golestan watershed demonstrated that the combination of geographic information systems and hydrological models can reveal the impact of physiographic and climatic factors on flood potential. The researchers also found that a sub-basin with a larger area or higher peak

discharge does not necessarily have a greater impact on the total watershed runoff, but the spatial location of sub-basin and river routing also play significant roles. In the current study, the clustering method have been used to determine the flood potential of the sub-basins of the Jiroft dam watershed. The values of curve number and time of concentration for each sub-basin are specified in Table 3.

Table 3. Curve number values and time of concentration in Jiroft dam catchment

| No. | Sub-basin | CN | time of concentration (min) | No. | Sub-basin | CN | time of concentration (min) |
|-----|-----------|------|-----------------------------|-----|-----------|------|-----------------------------|
| 1 | a1 | 82.1 | 42 | 23 | k20 | 77 | 27.5 |
| 2 | a2 | 81.3 | 35.38 | 24 | k3 | 77.1 | 33.83 |
| 3 | a3 | 90.1 | 52 | 25 | k4 | 78.1 | 41 |
| 4 | a4 | 87.1 | 35.83 | 26 | k5 | 91.1 | 39.17 |
| 5 | a5 | 82.1 | 68.67 | 27 | k6 | 94.1 | 41 |
| 6 | aroods | 78 | 35.5 | 28 | k7 | 88.1 | 47.83 |
| 7 | cheshmeh | 75.2 | 40.83 | 29 | k8 | 90.1 | 44.17 |
| 8 | H1 | 73.1 | 42.67 | 30 | k9 | 92.1 | 71.33 |
| 9 | h2 | 75 | 17.37 | 31 | konaroi | 84.1 | 59.33 |
| 10 | hanjan | 92 | 36.83 | 32 | maidan | 90.1 | 68.67 |
| 11 | k1 | 84.1 | 40.33 | 33 | n1 | 82.1 | 75.53 |
| 12 | k10 | 88 | 64.17 | 34 | n2 | 78.1 | 67.02 |
| 13 | k11 | 93.1 | 47.83 | 35 | n3 | 77.2 | 67.17 |
| 14 | k12 | 78.1 | 35.5 | 36 | n4 | 74.1 | 64.08 |
| 15 | k13 | 88.1 | 28.17 | 37 | n5 | 67.8 | 85.38 |
| 16 | k14 | 84.3 | 40.5 | 38 | narab | 74.4 | 33.5 |
| 17 | k15 | 82.1 | 35.5 | 39 | p1 | 73.2 | 70.6 |
| 18 | k16 | 76.5 | 34.33 | 40 | pol-baft | 87.1 | 52.17 |
| 19 | k17 | 78.5 | 31.17 | 41 | raman | 83.1 | 42.67 |
| 20 | k18 | 91.1 | 28.93 | 42 | s1 | 84.2 | 41.33 |
| 21 | k19 | 88.1 | 34.17 | 43 | soltani | 84.5 | 46.3 |
| 22 | k2 | 79.2 | 31.17 | | | | |

2.3.1. K-means clustering

Data clustering approach has been used for ranking the flood levels. There are several clustering techniques available, with K-means being one of the most commonly used methods. However, it is important to

note that K-means can be heavily influenced by the number of clusters chosen and the initial data provided. The value of K in K-means clustering is used to categorize the levels of flood intensity. For instance, a level

of 0 suggests that there is no risk of flooding, while a level of K signifies a high alert for the area under impact. The upcoming

algorithm describes the definition of predate and the clustering method [6].

Algorithm2. K-means clustering algorithm

Require: K, number of clusters; D, a data set of N points

Ensure: A set of K clusters

1. Data points: A set of individual data points is scattered throughout the diagram.
2. Centroids: K number of centroid points are initialized at random locations within the data points.
3. Cluster assignments: Each data point is assigned to the nearest centroid, forming K clusters.
4. Centroid update: The centroids are updated by calculating the mean of the data points in each cluster.
5. Iteration: The process of assigning data points to clusters and updating centroids is repeated until convergence, i.e., when the centroids no longer change significantly between iterations.

Determining the optimal number of clusters is important. In this study, the Silhouette coefficient was used to determine the optimal number of clusters due to its efficiency and simplicity of implementation in MATLAB software. Using this coefficient, the degree of membership of each data point to the cluster, it belongs to is measured.

2.3.1.1. Silhouette Method

The Silhouette method was first introduced by Peter.J. Rousseeuw[23]. The Silhouette method is widely used in determining k value or the number of clusters. K value is determined by the average Silhouette coefficients. For points in i in cluster A, the formula of s(i) for i in cluster from Silhouette of i is as follows:

$$s(i) = \frac{b(i)-a(i)}{\max\{a(i),b(i)\}}, \quad -1 \leq s(i) \leq 1 \quad (1)$$

Where: s(i) represents the coefficient indicating the level of membership of a data item (e.g., data i to its respective cluster (e.g., cluster A) following the cluster operation. Meanwhile, a(i) signifies the average distance of data i from other data items within cluster A, and b(i) denotes the smallest average distance of data i within cluster A to other data items in any cluster E that differs from cluster A.

In practical terms, the silhouette coefficient is initially computed for each data item using the equation 1. Subsequently, the average silhouette coefficient $\bar{s}(k)$ is derived for all available data (n) within each cluster (k) through the utilization of equation 2.

$$\bar{s}(k) = 1/n \sum_{i=1}^n s(i) \quad (2)$$

Interpretation of different ranges of silhouette coefficient is presented in Table 4.

Table 4. Guide to interpretation of the silhouette coefficient[24]

| Type | Interval silhouette coefficient | Interpretation |
|------|---------------------------------|--|
| 1 | 0.71 – 1.0 | The strong structure has been discovered |
| 2 | 0.52 – 0.70 | Reasonable structure has been found |
| 3 | 0.26 – 0.50 | The weak structure may mock |
| 4 | < 0.25 | Not found substantial structure |

2.3.1.2. Data Normalization

Data normalization, also known as standardization of data, is the process of adjusting data values to a common scale)in the range of [0, 0.9] (in this context) in order to facilitate comparison of the data in different ranges.

$$z = 0.1 + 0.8 * \frac{x_i - x_{imin}}{x_{imax} - x_{imin}} \quad (3)$$

In which: z is the standardized variable, x_i is the initial variable, x_{imin} and x_{imax} are the minimum and maximum values of

variable x_i , respectively[25].

3. Results and Discussions

3.1. clustering Results

The results related to the effect of the number of clusters on the distance and silhouette coefficient are presented in table 5, as this algorithm is based on unsupervised methods, the silhouette coefficient has been used to find the best number of clusters. As can be seen, the best result is related to the number of 9 clusters.

Table 5. Distance and silhouette coefficient for number of clusters

| Number of clusters | silhouette coefficient | Distance in best fit |
|--------------------|------------------------|----------------------|
| 10 | 0.78 | 3.034 |
| 9 | 0.97 | 2.99 |
| 8 | 0.87 | 3.6 |
| 7 | 0.791 | 3.339 |
| 6 | 0.76 | 3.76 |
| 5 | 0.61 | 4.138 |

In Table 6, the results of clustering algorithm based on 9 clusters in the Jiroft dam basin are presented. In this table, cluster 1 sub-basins have the lowest potential for flood, while cluster 9 sub-basins have the highest flood potential. The results of the clustering algorithm differed from those obtained from the flood indicator f in some cases. This discrepancy arose because, in clustering method, in addition to the CN parameter, the time of concentration is also considered a very important parameter for prioritizing areas susceptible to flooding. This case, namely the impact of concentration time on determining the flood potential of a watershed, has been confirmed in the study by Saghafian and Farazjou[22]. Based on the results presented in Table 5, sub-basins k9, K10, and Maidan are placed in cluster 9. To select the most sensitive area, the results of the study by Solaimani Sarood et al.[19] have been used. The values of the

flood index f for sub-basins k9, K10, and Maidan are 0.64, 0.71, and 0.71 respectively. By comparing the results of the present study and the flood index values, the Maidan sub-basin was selected as the most sensitive area (Fig.5). Based on the hydrological soil map of the region, the majority of the soil in the Maidan sub-basin falls within hydrological groups B and C. The land use of Maidan is classified as rock-bare soil, with an average slope of 0.38% and curve number of 95.36. These characteristics clearly indicate that this sub-basin has a very high potential for flood generation. Furthermore, the short distance of this sub-basin to the Jiroft dam, in comparison to sub-basins K9 and K10, makes it a logical choice for identifying the most effective area for flood production in the Jiroft dam watershed. This analysis is entirely consistent with the results of the K-means algorithm and the findings of Solaimani Sarood et al. [19].

Table 6. Results of the clustering algorithm for different areas

| No. | sub basin | Cluster number | Distance to centerpoint | No. | sub basin | Cluster number | Distance to centerpoint |
|-----|-----------|----------------|-------------------------|-----|-----------|----------------|-------------------------|
| 1 | a1 | 4 | 0.059295 | 23 | k20 | 3 | 0.089571 |
| 2 | a2 | 4 | 0.061506 | 24 | k3 | 2 | 0.023408 |
| 3 | a3 | 7 | 0.088125 | 25 | k4 | 4 | 0.055273 |
| 4 | a4 | 2 | 0.044694 | 26 | k5 | 7 | 0.06575 |
| 5 | a5 | 5 | 0.04509 | 27 | k6 | 7 | 0.13227 |
| 6 | aroods | 2 | 0.006774 | 28 | k7 | 7 | 0.081976 |
| 7 | cheshmeh | 2 | 0.084785 | 29 | k8 | 7 | 0.013878 |
| 8 | H1 | 2 | 0.13482 | 30 | k9 | 9 | 0.066619 |
| 9 | h2 | 3 | 0.10365 | 31 | konarobie | 8 | 0.071905 |
| 10 | hanjan | 7 | 0.10549 | 32 | maidan | 9 | 0.008537 |
| 11 | k1 | 4 | 0.020741 | 33 | n1 | 5 | 0.082364 |
| 12 | k10 | 9 | 0.067605 | 34 | n2 | 5 | 0.03339 |
| 13 | k11 | 8 | 0.071905 | 35 | n3 | 5 | 0.078863 |
| 14 | k12 | 2 | 0.048246 | 36 | n4 | 6 | 0.12427 |
| 15 | k13 | 1 | 0.040151 | 37 | n5 | 6 | 0.18489 |
| 16 | k14 | 4 | 0.062834 | 38 | narab | 3 | 0.11547 |
| 17 | k15 | 4 | 0.078261 | 39 | p1 | 6 | 0.067764 |
| 18 | k16 | 2 | 0.027914 | 40 | pol-baft | 7 | 0.11381 |
| 19 | k17 | 2 | 0.072625 | 41 | raman | 4 | 0.038072 |
| 20 | k18 | 1 | 0.056001 | 42 | s1 | 4 | 0.064664 |
| 21 | k19 | 1 | 0.04972 | 43 | soltani | 4 | 0.076295 |
| 22 | k2 | 2 | 0.07181 | | | | |

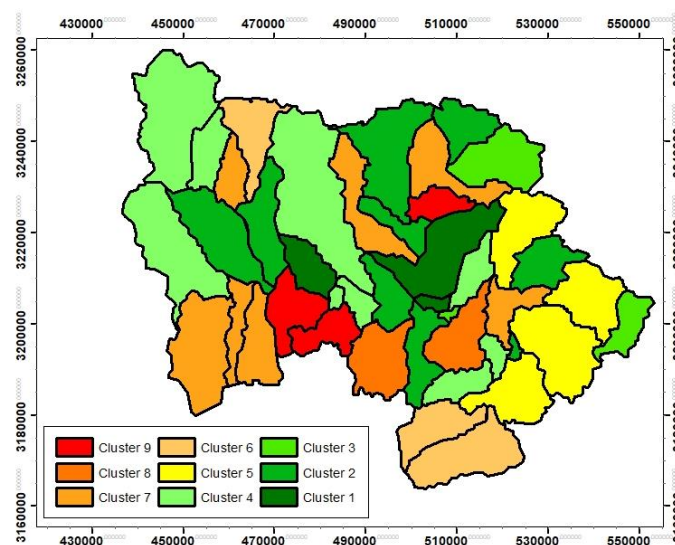


Figure 5. Clustering map of Jiroft dam basin

3.2. Geolocation results of IOT devices

The implementation of hexagonal algorithm in Jiroft dam basin is shown in

figure 6. After selecting the Maidan station as the most flood-prone area, this station is

chosen as the origin of coordinates and the x and y axes are drawn as described in Algorithm 1. Starting from the origin of coordinates, hexagons with a radius of 3.5 kilometers (equivalent to the WSN-03 module range) are drawn. The drawing of hexagons continues until the entire watershed area is covered. After drawing the hexagons, the coordinates of the centers of the hexagons are taken as the location for installing IoT equipment, then using the geographic information software ArcGIS, these coordinates are converted to Universal Transverse Mercator coordinate system(UTM). Based on this, the coordinates of 192 points for installing equipment were identified for the installation of equipment. The coordinates of these

points are presented in table 6 (due to the large number of points, only a few of them are presented in table 6).

Considering the costs of IoT devices, the implementation of this algorithm will lead to significant savings in installation and maintenance expenses, making the IoT-based flood prediction and warning system economically viable. Another important aspect to address is the energy saving for flood system. By implementing an algorithm to systematically shutdown and activation of devices, some of the IoT devices are put in sleep mode where the flood magnitude and probability of flooding is negligible. However, it is essential that the shutdown of the modules be conducted in a way that does not hinder data transmission and reception.

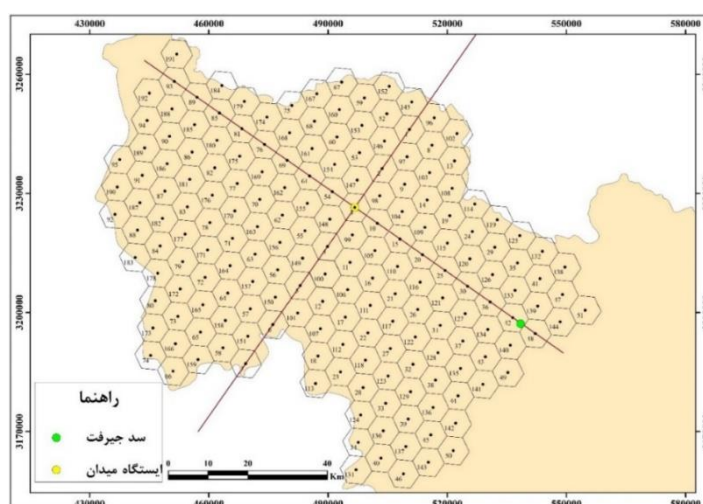


Figure 6. Implementation of the hexagonal algorithm in the Jiroft Dam catchment area

Table 7. Geographic coordinates of the IOT equipment installation location

| Location number | Utm(X) | Utm(Y) | Location number | Utm(X) | Utm(Y) | Location number | Utm(X) | Utm(Y) |
|-----------------|-----------|-----------|-----------------|-----------|-----------|-----------------|-----------|-----------|
| 1 | 510507.92 | 3246122.7 | 39 | 510205.99 | 3173130.2 | 78 | 460294.88 | 3222656.8 |
| 2 | 503633.24 | 3236287.1 | 40 | 503331.31 | 3163294.6 | 79 | 453420.2 | 3212821.2 |
| 3 | 496758.56 | 3226451.5 | 41 | 543383.29 | 3208503.4 | 80 | 446545.52 | 3202985.6 |
| 4 | 489883.88 | 3216616 | 42 | 536508.61 | 3198667.9 | 81 | 468365.66 | 3246297 |
| 5 | 483009.2 | 3206780.4 | 43 | 529633.93 | 3188832.3 | 82 | 461490.98 | 3236461.5 |
| 6 | 476134.52 | 3196944.8 | 44 | 522759.25 | 3178996.7 | 83 | 454616.3 | 3226625.9 |
| 7 | 469259.84 | 3187109.2 | 45 | 515884.57 | 3169161.1 | 84 | 447741.62 | 3216790.3 |
| 8 | 516186.5 | 3242153.6 | 46 | 509009.89 | 3159325.5 | 85 | 462687.08 | 3250266.1 |
| 9 | 509311.82 | 3232318 | 47 | 549061.87 | 3204534.3 | 86 | 455812.4 | 3240430.6 |

4. Conclusion

In flood warning systems, two important factors exist: the accuracy of flood detection and the speed of data transmission. The timely and rapid transmission of information in conventional flood warning systems may not be possible, therefore, in this study, internet of things (IoT)-based flood warning systems have been considered. One of the challenges in these systems is the optimal placement of equipment for data transmission in a way that ensures complete data collection without overlapping. In this study, a hexagonal algorithm was used for proper location placement of IoT devices in the Jiroft dam watershed. The first step in implementing the hexagonal algorithm is determining the most sensitive flood-prone area. For this purpose, two methods, K-means clustering and the flood index f , were utilized. By comparing the results of these two methods, the Maidan sub-basin was identified as the most sensitive sub-basin, with this sub-basin chosen as the coordinate

origin. Subsequently, hexagons were drawn with a radius of $R/2$ (the radius of the equipment's data transmission range) in a way that covered the entire watershed. The centers of these hexagons were determined, and local coordinates were transformed into UTM coordinates using ArcGIS software. In this study, the coordinates of 192 points were introduced for the installation of equipments. The results of this study will be useful in identifying challenges in the design and evaluation of IoT-based flood prediction and warning systems.

Acknowledgments

This study was funded by Regional water Company of Kerman (Grant numbers :402/04). The authors would like to thank to Kerman Regional Water Company (Research, Planning, and Economic Studies Department) for their financial support of this research.

References

1. Vaghefi SA, Keykhai M, Jahanbakhshi F, Sheikholeslami J, Ahmadi A, Yang, H, Abbaspour KC, (2019). The Future of Extreme Climate in Iran. *Scientific Reports* 9, Article 1464.
2. World Bank. (2019). Climate Knowledge Portal. [online] Available at: <https://climateknowledgeportal.worldbank.org/country/iran> [Accessed 9 Apr. 2019].
3. Yulindoko H, Subono S, Wardhani VA, Pramono Sh.H, Suwindarto P, (2018). Design of flood warning system based iot and water characteristics. *TELKOMNIKA (Telecommunication Computing Electronics and Control)*, 16(5), pp: 2101-2110.
4. Basha E, Rus D, (2007), Design of Early Warning Flood Detection Systems for Developing Countries. *International Conference on Information and Communication Technologies and Development*. Technologies and Development 2007 Dec 15, IEEE: 1-10.
5. Rani Dola Sh, Jayalakshmi GN, Baligar VP, (2020). Low cost IoT based flood monitoring system using machine learning and neural networks: flood alerting and rainfall prediction. *2nd International Conference on Innovative Mechanisms for Industry Applications (ICIMIA)*, pp: 261-267.
6. Sood SK, Sandhu R, Singla K, Chang V, (2018). IoT, big data and HPC based smart flood management framework. *Sustainable Computing: Informatics and Systems* 20, pp: 102-117.
7. Ancona M, Dellacasa A, Delzanno G, Camera AL, Rellini I, (2015). An "Internet of Things" vision of the flood monitoring problem. *InProc. 5th Int. Conf. Ambient Comput., Appl., Services Technol*, pp:26-29.
8. Udo EN, Isong EB, (2013). Flood monitoring and detection system using wireless sensor network. *Asian journal of computer and information systems*, 1(4).
9. Mousa, M., Zhang, X. and Claudel, C., 2016. Flash flood detection in urban cities using ultrasonic and infrared sensors. *IEEE Sensors Journal*, 16(19):7204-7216.

10. Madhumathi M, Grace R, (2017). Flood alert management system using iot and microcontroller. *International Journal of Innovative Research in Computer and Communication Engineering*, 5(4).
11. Hartono A, Satira S, Djamal M, Ramli M, (2017). Characterization Analysis of PVDF Thin Films Fabricated Using Deep Coating Machines. In *International Conference on Science and Technology-Promoting Sustainable Agriculture, Food Security, Energy, and Environment Through Science and Technology for Development*: 129-132.
12. Azid ShI, Sharma BN, Raghuvaiya K, Chand A, Prasad S, Jacquier A, (2015). SMS based flood monitoring and early warning system. *ARPN Journal of Engineering and Applied Sciences*, 10(15), pp: 6387-6391.
13. Shah WM, Arif FA, Shahrin A, Hassan A, (2018). The implementation of an IoT-based flood alert system. *International journal of advanced computer science and applications* 9(11).
14. Andrade MVA, Oishi S, (2014). A Wireless Mesh Sensor Network framework for river flood detection which can be used as a emergency communications network in case of disaster. 104, pp: 284.
15. Mitra P, Ray R, Chatterjee R, Basu R, Saha P, Raha S, Barman R, Patra S, Biswas SS, Saha S, (2016). Flood forecasting using Internet of things and artificial neural networks. *7th Annual Information Technology, Electronics and Mobile Communication Conference*: 1-5.
16. Bande S, Shete VV, (2017). Smart flood disaster prediction system using IoT and neural networks. *International Conference On Smart Technologies For Smart Nation (SmartTechCon)*, pp:189-194.
17. Shalini E, Surya P., Thirumurugan R, Subbulakshmi S, (2016). Cooperative flood detection using SMS through IoT. *Int. J. Adv. Res. Elect., Electron. Instrum. Eng.*, 5(3), pp: 3410-3414.
18. Zahir Sh, Ehkan B, Sabapathy Ph, Jusoh Th, Osman M, Yasin M.N, Wahab M N, et al. (2019). Smart IoT flood monitoring system. *Journal of physics: conference series*, 1339(1), 012043.
19. Solaimani Sarood F, Soltani Kopaii S, Salajeghe A, (2013). Selection of Appropriate Flooding Potential Index by Using RainfallRunoff (HEC-HMS) Model and RS & GIS Techniques in Jiroft Dam Basin, *Journal of Watershed Management Research*, 4(8), pp:90-105.
20. Sarai MH, Mahmoudi I, Bidsheki A, Kamandari M, (2017). A Study of the Geographical Distribution of Crimes in the Areas of Jiroft City Between 2008-2011. *Journal of Geography and Urban Planning Zagros Landscape*, 9(33), pp: 21-43.
21. Van Ackere S, Verbeurgt J, Sloover LD, Gautama S, Wulf AD, Maeyer Ph, (2019). A review of the internet of floods: Near real-time detection of a flood event and its impact. *Water* 11(11), pp: 2275.
22. Saghafian B, Farazjou H, (2007). Determination of place causing flood and respecting the floating of hydrologic units of Golestan Dam catchment. *Journal of Iran Watershed Management*, 1, pp:1-11, (In Persian).
23. Wulandari S, (2020). Analyze k-value selected method of k-means clustering algorithm to clustering province based on disease case. *International Journal of Innovative Technology and Exploring Engineering (IJITEE)*, 9(3), pp:121-124.
24. Sari BN, (2016). Identification of Tuberculosis Patient Characteristics Using K-Means Clustering. *Scientific Journal of Informatics*, 3(2), pp:129-138.
25. Tabatabaei M, Solaimani K, Habibnejad Roshan M, Kavian A, (2015). Estimation of Daily Suspended Sediment Concentration Using Artificial Neural Networks and Data Clustering by Self-Organizing Map (Case Study: Sierra Hydrometry Station- Karaj Dam Watershed) . *J Watershed Manage Res.* 5(10), pp: 98-116, (In Persian).

